Poly(*N*-isopropylacrylamide) Surfactant-Functionalized Responsive Silver Nanoparticles and Superlattices

Binsong Li,[†] Detlef-M. Smilgies,[‡] Andrew D. Price,[†,⊥] Dale L. Huber,[†,*] Paul G. Clem,[†] and Hongyou Fan[†,§,*]

[†]Sandia National Laboratories, Albuquerque, New Mexico 87185, United States, [‡]Cornell High Energy Synchrotron Source, Wilson Laboratory, Cornell University, Ithaca, New York 14853, United States, and [§]Center for Micro-Engineered Materials, Department of Chemical and Nuclear Engineering, University of New Mexico, Albuquerque, New Mexico 87131, United States [⊥]Present address: Senior Scientific, LLC, 800 Bradbury SE Suite 213, Albuquerque, New Mexico 87106, United States

ABSTRACT Metal nanoparticles exhibit unique optical characteristics in visible spectra produced by local surface plasmon resonance (SPR) for a wide range of optical and electronic applications. We report the synthesis of poly(*N*-isopropylacrylamide) surfactant (PNIPAM-C18)-functionalized metal nanoparticles and ordered superlattice arrays through an interfacial self-assembly process. The method is simple and reliable without using complex chemistry. The PNIPAM-C18-functionalized metal nanoparticles and ordered superlattices exhibit responsive behavior modulated by external temperature and relative humidity (RH). *In situ* grazing-incidence small-angle X-ray scattering studies confirmed that the superlattice structure of PNIPAM-C18 surfactant-functionalized nanoparticle arrays shrink and spring back reversibly based on external thermal and RH conditions, which allow flexible manipulation of interparticle spacing for tunable SPR. PNIPAM-C18 surfactants play a key role in accomplishing this responsive property. The ease of fabrication of the responsive nanostructure facilitates investigation of nanoparticle coupling that depends on interparticle separation for potential applications in chemical and biological sensors as well as energy storage devices.

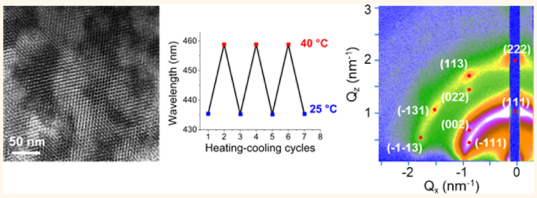

KEYWORDS: PNIPAM · silver nanoparticles · micelles · self-assembly · superlattice · responsive · GISAXS · SPR

Metal nanoparticles such as gold[1−3] and silver[4−6] nanoparticles exhibit unique optical properties in the visible spectrum produced by local surface plasmon resonance (SPR). Coupling of nearest neighbor nanoparticles within self-assembled arrays further results in new properties, so-called collective SPR,[7−10] which induces a shift of the plasmonic peaks or creates hot spots that depend on the interparticle distance.[11−14] These properties provide the essential and technological basis for fabrication of chemical and biological sensors, for chemical deposition, and for understanding charge or energy transfer between nanoparticles.[15,16] Precise control of interparticle spacing is required for efficient integration of this concept for the above applications. To this end, a wide range of efforts have been made to explore adjusting interparticle distance in order to tune the SPR.[17,18] Early efforts were focused on synthesis of monodisperse nanoparticles with controlled organic chain length.[19] Organic ligands on a nanoparticle surface play an important role in preventing nanoparticles from aggregating, which essentially enables control of interparticle spacing. Depending on the chain length, the interparticle distance can be varied when nanoparticles self-assemble into ordered arrays.[20] The advantage of this method is that the interparticle spacing can be precisely tuned at the atomic level using molecular alkane chains. For example, monodisperse gold nanoparticles were synthesized using alkanethiols ($CH_3(CH_2)_nSH$). The length of each $-CH_2$ group is ~1.2 Å. By changing the alkane length (*e.g.*, changing the *n* number), the overall interparticle spacing can be varied on the basis of 1.2 Å. The drawback of this method is that when the alkane chains are too short (*e.g.*, fewer than six $-CH_2$ groups), it is synthetically difficult to retain the monodispersity. Thus, the interparticle distance of the resulting nanoparticles are ill-defined, which limits the ability to tune the SPR. Moreover,

* Address correspondence to dlhuber@sandia.gov (D. Huber); hfan@sandia.gov (H. Fan).

Received for review February 4, 2014 and accepted April 6, 2014.

Published online April 07, 2014
10.1021/nn500690h

complicated chemistry is involved during synthesis, which often also results in poor quality control of the monodispersity of the functionalized nanoparticles. Additionally, tedious postseparation and purification make the final yield very low.

Driven to overcome the limitations, recent efforts were made to achieve dynamic and reversible tuning of the surface plasmon coupling. One way to accomplish this is to use organic ligands that respond to external environmental stimuli (*e.g.*, thermal or pH changes), in order to functionalize the nanoparticle surface (through chemical bonding) so that the interparticle spacing of the resulting functionalized nanoparticles varies in response to external temperature or pH changes.[2,21−24] Similarly, Liu *et al.* recently developed a thermoresponsive gold nanoparticle assembly for reversible tuning of surface plasmon coupling. This method relies on charge-stabilized gold nanoparticle assemblies.[25]

Here we developed a simple and reliable method to synthesize poly(*N*-isopropylacrylamide) (PNIPAM) derivative functionalized silver nanoparticle micelles and arrays that are responsive to external environmental changes.

RESULTS AND DISCUSSION

PNIPAM derivative functionalized silver nanoparticle micelles were synthesized through an interfacially driven microemulsion (μ-emulsion) method that we developed in the past.[26,27] In our previous work, μ-emulsions were fabricated through dispersion of an organic solution containing nanoparticles as the building blocks to another immiscible aqueous solution; subsequently, we removed the organic solvent through thermally driven evaporation, which induces nanoparticle self-assembly that was confined within μ-emulsion droplets.[12] The balanced interactions (van der Waals, dipole−dipole interactions, ligand−ligand attractions, *etc.*) between nanoparticles lead to formation of ordered nanostructured particle arrays. Herein, we extended this method to synthesize PNIPAM derivative functionalized silver nanoparticle micelles by using long alkyl chain substituted PNIPAM surfactant (PNIPAM-C18; see Scheme 1) and metal (gold and silver) nanoparticles that were functionalized with myristic acid or 1-dodecanethiol. In a general preparation, PNIPAM-C18 surfactant was added to deionized water to form solution A. Solution A was sonicated to

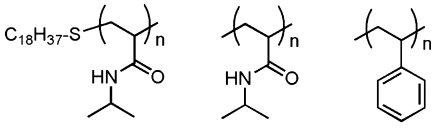

PNIPAM-C18 PNIPAM PS

Scheme 1. Molecular structures of PNIPAM-C18 surfactant, poly(*N*-isopropylacrylamide) (PNIPAM), and polystyrene (PS).

completely dissolve the PNIPAM-C18 surfactant. In another preparation, 5.5 nm silver nanoparticles were dissolved in 1−2 mL of chloroform to form solution B. Solutions A and B were mixed together with vigorous stirring, and the chloroform was removed by vacuum or heat treatment to complete the formation of silver PNIPAM-C18 nanoparticle (Ag-PNIPAM-C18) micelles in water. Due to the amphiphilic nature of the PNIPAM-C18 surfactant, the method is very simple and enables preparation of silver nanoparticle micelles without using chemical reactions. The resulting Ag-PNIPAM-C18 micelle solution is light brown and was diluted for UV−vis spectroscopy or TEM characterization. The micelle solution was very stable, and no visible precipitate was observed over 3 months. Self-assembly of these silver nanoparticle micelles can further form ordered arrays that respond to external temperature changes. *In situ* grazing-incidence small-angle X-ray scattering (GISAXS) was carried out to monitor the evolution of interparticle spacing changes during a thermal cycling process.[28]

Figure 1A,B show representative transmission electron micrograph (TEM) images of Ag nanoparticle micelles. Dynamic light scattering measurements (Figure S1) show a similar narrow size distribution to the Ag nanoparticles. Formation of ordered hexagonal (A) and cubic lattice (B) arrays confirmed the monodispersity of the Ag nanoparticle micelles. The GISAXS image (Figure 1C) of the ordered Ag nanoparticle micelle arrays prepared by drying the stock solution on a Si wafer exhibits face centered cubic (fcc) lattice patterns. On the basis of fcc symmetry, the primary peaks in line scan pattern (Figure 1D) could be assigned as corresponding to the 111, 200, 220, and 311 Bragg planes. The calculated unit cell parameter a = 114.3 Å.

The thermoresponsive properties of Ag-PNIPAM-C18 micelles was studied by UV−vis absorption spectroscopy, and the result is shown in Figure 2A. At 25 °C, the aqueous micelle solution was transparent. Upon heating the micelle solution to above 32 °C (lower critical solution temperature, LCST),[29−31] the solution became cloudy due to the coil-to-globule transition of the PNIPAM-C18 chain, which caused light scattering in the aqueous phase. The plasmon peak red-shifted from 435.2 nm to 458.9 nm. This is likely due to the result of the decreasing of interparticle distance caused by the shrinkage of PNIPAM-C18 and the increasing of the refractive index of PNIPAM-C18 chain segments surrounding the Ag NPs at increased temperature. Upon cooling from 40 °C to 25 °C, the plasmon peak shifted back to 435.2 nm. This process was fully reversible during heating−cooling cycles between 25 and 40 °C as shown in Figure 2B,C.

The thermoresponsive behavior of thin films of Ag-PNIPAM-C18 micelle arrays was studied with GISAXS during the thermal cycling processes. In order to study

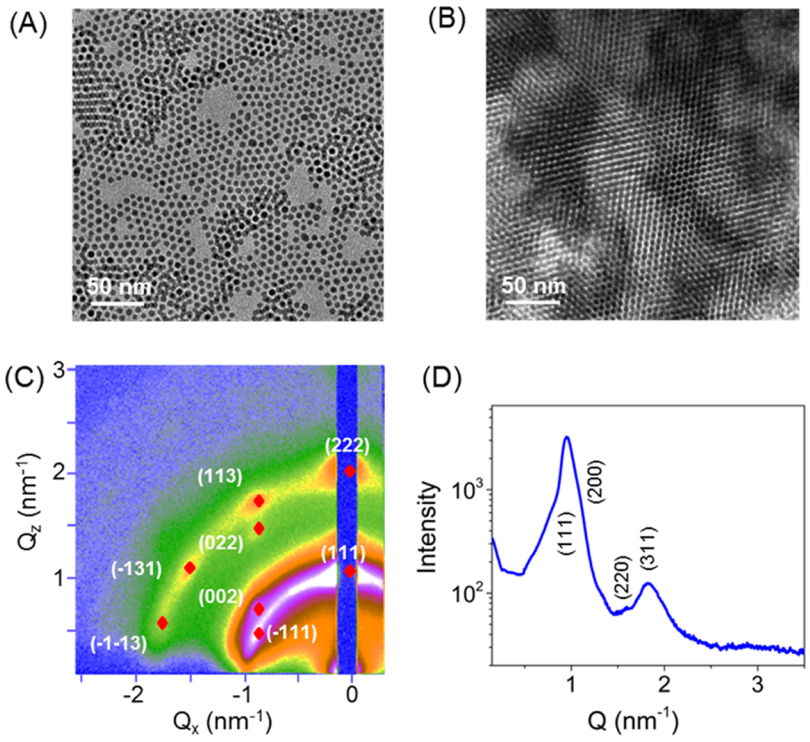

Figure 1. Characterization of Ag nanoparticle micelles and ordered arrays. Representative transmission electron micrographs (TEM) of individual Ag nanoparticle micelles (A) and ordered arrays (B). (C) Representative GISAXS image of ordered Ag nanoparticle micelle arrays at room temperature and RH of 44% and (D) a 2D line cut obtained from the image in (C).

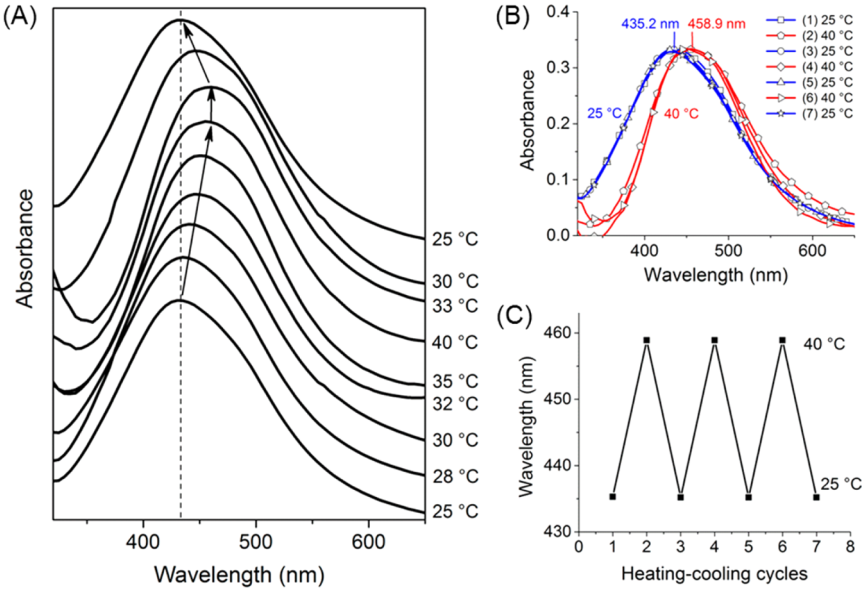

Figure 2. Responsive optical property of PNIPAM-C18-functionalized Ag nanoparticle micelle in water. (A) UV−vis spectra of the aqueous solution of Ag-PNIPAM-C18 micelles during increasing and decreasing temperature and (B) during a reversible heating and cooling process. (C) Reversible changes of Ag nanoparticle SPR peak during heating and cooling cycles in (B).

the change of the lattice constant at various temperatures, thin films of ordered Ag-PNIPAM-C18 micelle arrays were prepared on Si wafers and were placed on a thermal stage in a sealed chamber with controlled temperature. GISAXS measurements were carried out to monitor the superlattice structural evolution during the thermal cycling process. Figure 3 shows the GISAXS results from the thermal cycling of thin films of Ag-PNIPAM-C18 micelle arrays at different temperatures. The Ag-PNIPAM-C18 micelles formed a cubic, fcc superlattice at 25 °C, with a lattice parameter *a* of 114.3 Å (Figure 3A). When the temperature was increased to 40 °C, all the peaks from SAXS patterns shifted to a smaller *d*-spacing. The overall dimensions of the fcc lattice shrank as indicated by the shrinkage of the d_{111} spacing (Figure 3B). This further caused

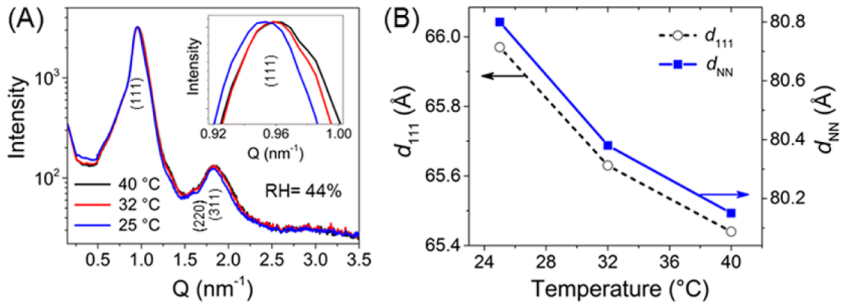

Figure 3. Responsive behavior of Ag nanoparticle arrays at varied temperature. (A) 2D line cut GISAXS patterns of a film of Ag-PNIPAM-C18 arrays at varied temperature. (B) d_{111} spacing and interparticle spacing d_{NN} calculated from GISAXS patterns in (A) at the corresponding temperature.

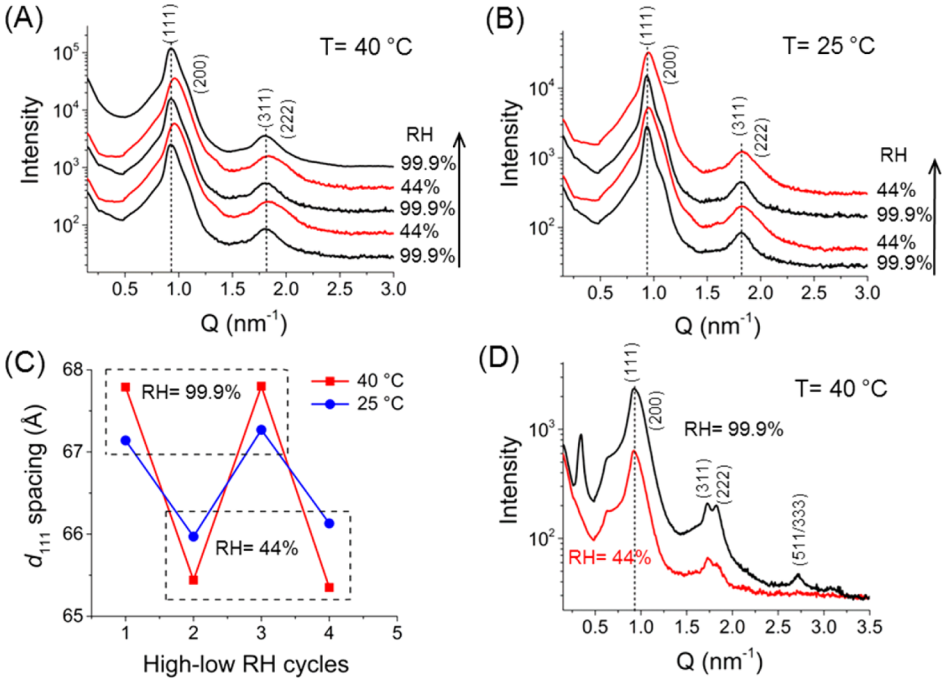

Figure 4. Responsive behavior of Ag-PNIPAM-C18 micelle arrays at varied RH. (A) GISAXS patterns of Ag-PNIPAM-C18 arrays under different RH at 40 °C. (B) GISAXS spectra of Ag-PNIPAM-C18 arrays under different RH at 25 °C. (C) d_{111} spacing of a Ag-PNIPAM-C18 micelle array. (D) GISAXS spectra of Au-PS arrays under different RH at 40 °C.

the interparticle distance d_{NN} to shrink (Figure 3B). This is likely due to the thermoresponsive nature of PNIPAM-C18 around the Ag nanoparticle surface. When the temperature is above the LCST, PNIPAM-C18 chains shrink due to coil-to-globule transition, which leads to overall shrinkage of the lattice dimension of Ag-PNIPAM-C18 micelle arrays.

In addition to the thermoresponsive behavior, we also found out that Ag-PNIPAM-C18 micelle arrays exhibit another responsive property due to the external environment. The spatial lattice dimension of Ag-PNIPAM-C18 micelle arrays changes according to external relative humidity (RH). During controlled experiments, the thin films of Ag-PNIPAM-C18 arrays were placed in a sealed chamber with controlled temperature and RH. GISAXS was carried out to monitor structural evolution of the Ag-PNIPAM-C18 superlattice. At the beginning of the experiments, the lattice structure exhibits an fcc cubic superlattice structure with a lattice parameter a of 117.5 Å at 40 °C and RH of 99.9%. When the RH inside the chamber was lowered to ~44%, all the peaks in the SAXS patterns shifted to smaller d-spacing, as shown in Figure 4A. This suggests that the superlattice dimension shrunk while the RH decreased. The calculated lattice parameter a changed to 113.4 Å. When the RH in the chamber was raised back to 99%, the GISXAS patterns returned to their original positions, which indicates that the shrunken superlattices sprang back. Experiments at different temperatures showed similar shrinkage and spring-back behavior (Figure 4B). We found that the shrinkage and spring-back processes of the Ag-PNIPAM-C18 superlattice structure are reversible (Figure 4C). To further confirm the function of the PNIPAM-C18 surfactant surrounding nanoparticles, similar experiments were performed using thin films of nanoparticle arrays

with polystyrene instead of PNIPAM-C18 surfactant as a comparison. The GISAXS patterns (Figure 4D) from these films showed no shift when the RH was changed back and forth. This suggests that the external RH has no influence on the superlattice structure of the nanoparticle arrays. It unambiguously establishes that PNIPAM-C18 plays a key role in inducing lattice responsiveness to external RH.

CONCLUSION

In summary, we prepared PNIPAM-C18-functionalized metal nanoparticles and ordered superlattice arrays through an interfacial self-assembly processes. The method is simple and reliable without using complex chemistry. The Ag-PNIPAM-C18 nanoparticles and ordered superlattices exhibit responsive behavior modulated by external temperature and RH. GISAXS studies confirmed that the superlattice structure of PNIPAM-C18 surfactant functionalized nanoparticle arrays shrinks and springs back reversibly based on external thermal and RH conditions, which allows flexible manipulation of interparticle spacing for tunable SPR. PNIPAM-C18 surfactants play a key role in accomplishment of the responsive property. The ease of fabrication of the responsive nanostructure facilitates investigation of nanoparticle coupling that depends on interparticle separation for potential applications in chemical and biological sensors as well as energy storage devices.

METHODS

Materials. Polystyrene (PS) was purchased from Aldrich. The PNIPAM-C18 was synthesized by free radical polymerization in the presence of octadecanethiol, which acted as a chain transfer agent. The myristate-protected silver (Ag)[32,33] and gold (Au)[34] nanoparticles capped with 1-dodecanethiol were synthesized according to literature methods. The standard size distribution is ~5%.

Preparation of Ag-PNIPAM-C18 Micelles and Ordered Arrays. In a general preparation, PNIPAM-C18 surfactant was added to deionized water to form solution A. Solution A was sonicated to completely dissolve the PNIPAM surfactant. In another preparation, 5.5 nm silver nanoparticles were dissolved in 1−2 mL of chloroform to form solution B. Solutions A and B were mixed together with vigorous stirring, and the chloroform was removed by vacuum or heat treatment to complete the formation of silver PNIPAM-C18 nanoparticle (Ag-PNIPAM-C18) micelles in water. Specifically, Ag nanoparticles (40 mg) were dispersed in 0.8 mL of chloroform and added into an aqueous PNIPAM-C18 solution (45 mg in 1 mL of DI water). The mixture was shaken vigorously. The chloroform was allowed to evaporate slowly while the mixture was stirred at 800 rpm and heated at 50 °C. The colorless aqueous phase became brownish after the chloroform was gone, which indicated the formation of Ag-PNIPAM-C18 micelles.[35] The resulting suspension was centrifuged at 4000 rpm for 2 min to remove large clusters, and a clear brown aqueous solution of Ag-PNIPAM-C18 micelles was obtained. To prepare Ag-PNIPAM-C18 arrays, Ag-PNIPAM-C18 micelle solutions were dropcast on a Si wafer and allowed to dry slowly at 40 °C.

Characterization. Transmission electron microscopy was performed on a JEOL 2010 with a 200 kV acceleration voltage, equipped with a Gatan slow scan CCD camera. UV−vis spectra were obtained on a Lambda 950 spectrophotometer (PerkinElmer). Grazing-incidence small-angle X-ray scattering[36] was performed on the D1 station at the Cornell High Energy Synchrotron Source using monochromatic radiation of wavelength λ = 1.1688 Å. The sample to detector distance was 603.3 mm, as determined using a silver behenate powder standard. The incident angle of the X-ray beam was varied from 0.1° to 0.5°. Typical exposure times ranged from 0.1 to 2.0 s. Scattering images were calibrated and integrated using the Fit2D software. Dynamic light scattering (DLS) was measured on a Zetasizer Nano S, Malvern.

Conflict of Interest: The authors declare no competing financial interest.

Acknowledgment. This work was supported by the U.S. Department of Energy, Office of Basic Energy Sciences, Division of Materials Sciences and Engineering. TEM studies were performed in the Department of Earth and Planetary Sciences at University of New Mexico. Part of this work is based upon research conducted at the Cornell High Energy Synchrotron Source (CHESS), which is supported by the National Science Foundation and the National Institutes of Health/National Institute of General Medical Sciences under NSF award DMR-0936384. Sandia National Laboratories is a multiprogram laboratory managed and operated by Sandia Corporation, a wholly owned subsidiary of Lockheed Martin Corporation, for the U.S. Department of Energy's National Nuclear Security Administration under contract DE-AC04-94AL85000.

Supporting Information Available: DLS data of the Ag nanoparticles and micelles. This material is available free of charge via the Internet at http://pubs.acs.org.

REFERENCES AND NOTES

1. Xu, H. X.; Xu, J.; Zhu, Z. Y.; Liu, H. W.; Liu, S. Y. *In-Situ* Formation of Silver Nanoparticles with Tunable Spatial Distribution at the Poly(N-Isopropylacrylamide) Corona of Unimolecular Micelles. *Macromolecules* **2006**, *39*, 8451–8455.
2. Zhao, X. L.; Ding, X. B.; Deng, Z. H.; Zheng, Z. H.; Peng, Y. X.; Tian, C. R.; Long, X. P. A Kind of Smart Gold Nanoparticle-Hydrogel Composite with Tunable Thermo-Switchable Electrical Properties. *New J. Chem.* **2006**, *30*, 915–920.
3. Lica, G. C.; Zelakiewicz, B. S.; Constantinescu, M.; Tong, Y. Y. Charge Dependence of Surface Plasma Resonance on 2 nm Octanethiol-Protected Au Nanoparticles: Evidence of a Free-Electron System. *J. Phys. Chem. B* **2004**, *108*, 19896–19900.
4. Alvarez-Puebla, R. A.; Contreras-Caceres, R.; Pastoriza-Santos, I.; Perez-Juste, J.; Liz-Marzan, L. M. Au@PNIPAM Colloids as Molecular Traps for Surface-Enhanced, Spectroscopic, Ultra-Sensitive Analysis. *Angew. Chem. Int., Ed.* **2009**, *48*, 138–143.
5. Wu, T.; Ge, Z. S.; Liu, S. Y. Fabrication of Thermoresponsive Cross-Linked Poly(N-Isopropylacrylamide) Nanocapsules and Silver Nanoparticle-Embedded Hybrid Capsules with Controlled Shell Thickness. *Chem. Mater.* **2011**, *23*, 2370–2380.
6. Choi, B. H.; Lee, H. H.; Jin, S. M.; Chun, S. K.; Kim, S. H. Characterization of the Optical Properties of Silver Nanoparticle Films. *Nanotechnology* **2007**, *18*, 075706.
7. Sih, B. C.; Wolf, M. O. Dielectric Medium Effects on Collective Surface Plasmon Coupling Interactions in Oligothiophene-Linked Gold Nanoparticles. *J. Phys. Chem. B* **2006**, *110*, 22298–22301.
8. Pinchuk, A. O.; Schatz, G. C. Collective Surface Plasmon Resonance Coupling in Silver Nanoshell Arrays. *Appl. Phys. B: Lasers Opt.* **2008**, *93*, 31–38.

9. Chiu, C. S.; Chen, H. Y.; Hsiao, C. F.; Lin, M. H.; Gwo, S. Ultrasensitive Surface Acoustic Wave Detection of Collective Plasmonic Heating by Close-Packed Colloidal Gold Nanoparticles Arrays. *J. Phys. Chem. C* **2013**, *117*, 2442–2448.
10. Toma, M.; Toma, K.; Michioka, K.; Ikezoe, Y.; Obara, D.; Okamotod, K.; Tamadaw, K. Collective Plasmon Modes Excited on a Silver Nanoparticle 2D Crystalline Sheet. *Phys. Chem. Chem. Phys.* **2011**, *13*, 7459–7466.
11. Halas, N. J.; Lal, S.; Chang, W. S.; Link, S.; Nordlander, P. Plasmons in Strongly Coupled Metallic Nanostructures. *Chem. Rev.* **2011**, *111*, 3913–3961.
12. Tian, L. M.; Chen, E.; Gandra, N.; Abbas, A.; Singamaneni, S. Gold Nanorods as Plasmonic Nanotransducers: Distance-Dependent Refractive Index Sensitivity. *Langmuir* **2012**, *28*, 17435–17442.
13. Wang, X. L.; Gogol, P.; Cambril, E.; Palpant, B. Near- and Far-Field Effects on the Plasmon Coupling in Gold Nanoparticle Arrays. *J. Phys. Chem. C* **2012**, *116*, 24741–24747.
14. Park, J. S.; Yoon, J. H.; Yoon, S. Spatially Controlled Sers Patterning Using Photoinduced Disassembly of Gelated Gold Nanoparticle Aggregates. *Langmuir* **2010**, *26*, 17808–17811.
15. Kumar, G. V. P. Plasmonic Nano-Architectures for Surface Enhanced Raman Scattering: A Review. *J. Nanophotonics* **2012**, *6*, 064503.
16. Du, Y. C.; Shi, L. N.; Hong, M. H.; Li, H. L.; Li, D. M.; Liu, M. A Surface Plasmon Resonance Biosensor Based on Gold Nanoparticle Array. *Opt. Commun.* **2013**, *298*, 232–236.
17. Jain, P. K.; Huang, W. Y.; El-Sayed, M. A. On the Universal Scaling Behavior of the Distance Decay of Plasmon Coupling in Metal Nanoparticle Pairs: A Plasmon Ruler Equation. *Nano Lett.* **2007**, *7*, 2080–2088.
18. Lange, H.; Juarez, B. H.; Carl, A.; Richter, M.; Bastus, N. G.; Weller, H.; Thomsen, C.; von Klitzing, R.; Knorr, A. Tunable Plasmon Coupling in Distance-Controlled Gold Nanoparticles. *Langmuir* **2012**, *28*, 8862–8866.
19. Choi, J. J.; Luria, J.; Hyun, B. R.; Bartnik, A. C.; Sun, L.; Lim, Y. F.; Marohn, J. A.; Wise, F. W.; Hanrath, T. Photogenerated Exciton Dissociation in Highly Coupled Lead Salt Nanocrystal Assemblies. *Nano Lett.* **2010**, *10*, 1805–1811.
20. Chen, C. F.; Tzeng, S. D.; Chen, H. Y.; Lin, K. J.; Gwo, S. Tunable Plasmonic Response from Alkanethiolate-Stabilized Gold Nanoparticle Superlattices: Evidence of Near-Field Coupling. *J. Am. Chem. Soc.* **2008**, *130*, 824–826.
21. Contreras-Caceres, R.; Sanchez-Iglesias, A.; Karg, M.; Pastoriza-Santos, I.; Perez-Juste, J.; Pacifico, J.; Hellweg, T.; Fernandez-Barbero, A.; Liz-Marzan, L. M. Encapsulation and Growth of Gold Nanoparticles in Thermoresponsive Microgels. *Adv. Mater.* **2008**, *20*, 1666–1670.
22. Li, D. X.; He, Q.; Yang, Y.; Mohwald, H.; Li, J. B. Two-Stage pH Response of Poly(4-Vinylpyridine) Grafted Gold Nanoparticles. *Macromolecules* **2008**, *41*, 7254–7256.
23. Tokareva, I.; Minko, S.; Fendler, J. H.; Hutter, E. Nanosensors Based on Responsive Polymer Brushes and Gold Nanoparticle Enhanced Transmission Surface Plasmon Resonance Spectroscopy. *J. Am. Chem. Soc.* **2004**, *126*, 15950–15951.
24. Tang, F.; Ma, N.; Wang, X. Y.; He, F.; Li, L. D. Hybrid Conjugated Polymer-Ag@PNIPAM Fluorescent Nanoparticles with Metal-Enhanced Fluorescence. *J. Mater. Chem.* **2011**, *21*, 16943–16948.
25. Liu, Y. D.; Han, X. G.; He, L.; Yin, Y. D. Thermoresponsive Assembly of Charged Gold Nanoparticles and Their Reversible Tuning of Plasmon Coupling. *Angew. Chem. Int., Ed.* **2012**, *51*, 6373–6377.
26. Fan, H. Y. Nanocrystal-Micelle: Synthesis, Self-Assembly and Application. *Chem. Commun.* **2008**, 1383–1394.
27. Fan, H. Y.; Leve, E. W.; Scullin, C.; Gabaldon, J.; Tallant, D.; Bunge, S.; Boyle, T.; Wilson, M. C.; Brinker, C. J. Surfactant-Assisted Synthesis of Water-Soluble and Biocompatible Semiconductor Quantum Dot Micelles. *Nano Lett.* **2005**, *5*, 645–648.
28. Dunphy, D.; Fan, H. Y.; Li, X. F.; Wang, J.; Brinker, C. J. Dynamic Investigation of Gold Nanocrystal Assembly Using *in Situ* Grazing-Incidence Small-Angle X-Ray Scattering. *Langmuir* **2008**, *24*, 10575–10578.
29. Kogure, H.; Nanami, S.; Masuda, Y.; Toyama, Y.; Kubota, K. Hydration and Dehydration Behavior of N-Isopropylacrylamide Gel Particles. *Colloid Polym. Sci.* **2005**, *283*, 1163–1171.
30. Wu, C.; Wang, X. H. Globule-to-Coil Transition of a Single Homopolymer Chain in Solution. *Phys. Rev. Lett.* **1998**, *80*, 4092–4094.
31. Schild, H. G. Poly (N-Isopropylacrylamide) - Experiment, Theory and Application. *Prog. Polym. Sci.* **1992**, *17*, 163–249.
32. Yamamoto, M.; Nakamoto, M. Novel Preparation of Monodispersed Silver Nanoparticles *via* Amine Adducts Derived from Insoluble Silver Myristate in Tertiary Alkylamine. *J. Mater. Chem.* **2003**, *13*, 2064–2065.
33. Richards, V. N.; Rath, N. P.; Buhro, W. E. Pathway from a Molecular Precursor to Silver Nanoparticles: The Prominent Role of Aggregative Growth. *Chem. Mater.* **2010**, *22*, 3556–3567.
34. Zheng, N.; Fan, J.; Stucky, G. D. One-Step One-Phase Synthesis of Monodisperse Noble-Metallic Nanoparticles and Their Colloidal Crystals. *J. Am. Chem. Soc.* **2006**, *128*, 6550–6551.
35. Fan, H. Y.; Yang, K.; Boye, D. M.; Sigmon, T.; Malloy, K. J.; Xu, H. F.; Lopez, G. P.; Brinker, C. J. Self-Assembly of Ordered, Robust, Three-Dimensional Gold Nanocrystal/Silica Arrays. *Science* **2004**, *304*, 567–571.
36. Di, Z.; Posselt, D.; Smilgies, D. M.; Papadakis, C. M. Structural Rearrangements in a Lamellar Diblock Copolymer Thin Film During Treatment with Saturated Solvent Vapor. *Macromolecules* **2010**, *43*, 418–427.